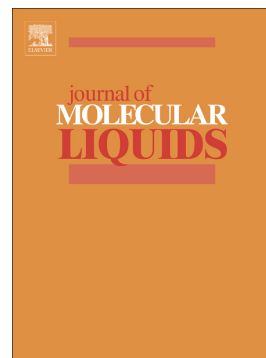


## Accepted Manuscript

Synthesis and surface functionalization of multi-walled carbon nanotubes with imidazolium and pyridinium-based ionic liquids: Thermal stability, dispersibility and hydrophobicity characteristics



Mzukisi Matandabuzo, Peter A. Ajibade

PII: S0167-7322(18)32558-3  
DOI: doi:[10.1016/j.molliq.2018.07.028](https://doi.org/10.1016/j.molliq.2018.07.028)  
Reference: MOLLIQ 9349  
To appear in: *Journal of Molecular Liquids*  
Received date: 18 May 2018  
Revised date: 6 July 2018  
Accepted date: 7 July 2018

Please cite this article as: Mzukisi Matandabuzo, Peter A. Ajibade , Synthesis and surface functionalization of multi-walled carbon nanotubes with imidazolium and pyridinium-based ionic liquids: Thermal stability, dispersibility and hydrophobicity characteristics. Molliq (2018), doi:[10.1016/j.molliq.2018.07.028](https://doi.org/10.1016/j.molliq.2018.07.028)

This is a PDF file of an unedited manuscript that has been accepted for publication. As a service to our customers we are providing this early version of the manuscript. The manuscript will undergo copyediting, typesetting, and review of the resulting proof before it is published in its final form. Please note that during the production process errors may be discovered which could affect the content, and all legal disclaimers that apply to the journal pertain.

**Synthesis and surface functionalization of multi-walled carbon nanotubes with imidazolium and pyridinium-based Ionic Liquids: Thermal stability, dispersibility and hydrophobicity characteristics**

**Mzukisi Matandabuzo, Peter A. Ajibade\***

*School of Chemistry and Physics, University of KwaZulu-Natal, Private Bag X01, Scottsville, Pietermaritzburg 3209, South Africa*

**Abstract**

Functionalized multi-walled carbon nanotubes (MWCNTs) were synthesized by simple chemical method, and dispersed using imidazolium and pyridinium-based ionic liquids (ILs). The as-synthesized ILs-MWCNT composites were studied using FTIR spectroscopy, scanning electron microscopy (SEM), energy dispersive X-ray spectroscopy (EDS), thermogravimetric analysis (TGA), and solubility in different polar and non-polar solvents. Spectroscopic and microscopy analyses confirmed the formation of the ILs-MWCNT composites with new functionalities. Spectra studies showed graphitic and carboxylic groups in the pure MWCNTs. MWCNTs SEM images showed entangled bundles, while ILs-MWCNTs showed debundled composites with increased diameter and unaltered MWCNTs morphology. TGA indicates that the MWCNTs are thermally stable which could be ascribed to *Van der Waals* and non-covalent interactions within the composites matrices. Solubility studies indicates the ILs-MWCNT composites are hydrophobic behaviour, insoluble in water and other polar solvents.

**KEYWORDS:** Carbon nanotubes; ionic liquids; imidazolium; pyridinium; functionalization.

\*Corresponding author Email: [ajibadep@ukzn.ac.za](mailto:ajibadep@ukzn.ac.za)

## 1. Introduction

Ionic liquids (ILs) (also known as electrolytes), are organic/inorganic salts made up of large and asymmetric ions with delocalized charges and different chemical functional groups [1-3]. ILs exists in liquid form at room temperature with melting point lower than 100 °C [4-5]. ILs possesses special properties such as non-volatility, good thermal stability, low melting point, and relatively good electrical conductivity [5]. ILs has been used as solvents and potential stabilizers for various nanoparticles used in catalysis and material science [6-7]. ILs are being used in different applications such as electrochemical energy and electrochemical double-layer capacitors (EDCLs) [4, 8-12]. The incorporation and/or coating of carbon nanotubes with different salts, nanoparticles, polymers, and ionic liquids produces composites with enhanced physical, chemical and mechanical stability that can be easily process and hydrophobic [13]. The formation of bucky gels is known as the first discovery of ionic liquids/carbon nanotubes composites [14-17]. However, due to the presence of highly polarizable  $\pi$  electrons in ionic liquids, the interactions between the carbon-based  $\pi$ -systems and ionic liquids are very complex [15]. Espejo *et al.*, [18] reported the dispersion of multi-walled carbon nanotubes (MWCNTs) in imidazolium-based ILs to produce stable and homogeneous dispersions with relatively new and unique properties. It was also reported that dispersion of CNTs in ILs produces composites with enhanced surface area [18]. Yang *et al.* [19] reported the functionalization of MWCNTs with 2,2'-(ethylenedioxy)-diethylamine, 1,8-diaminooctane, and pristine. They observed that MWCNTs functionalized with 2,2'-

(ethylendioxy)-diethylamine were individually integrated into the epoxy matrix, whereas MWCNTs with 1,8-diaminooctane were poorly dispersed with notable weak interface adhesion. Salam & Burk [20] reported the synthesis and functionalization of multi-walled carbon nanotubes by octadecylamine (ODA) and polyethylene glycol (PEG). Their results revealed that only 16% (wt) of MWCNTs was covered by PEG, while 39% (wt) was covered by ODA. The dispersion of MWCNTs in polymer composites was reported by Pereira *et al.*, [21], in their preliminary study of MWCNTs in poly(vinylidene fluoride), MWCNT/PVDF/ZrO<sub>2</sub>. Spectra studies of the synthesized nanocomposites confirmed the incorporation of the MWCNTs into poly(vinylidene fluoride) matrix [21].

Ohba and Chaban [22] reported the structure and dynamics of imidazolium-based ILs confined inside carbon nanotubes. França [15] reported that CNTs covalently modified with imidazolium-based ILs are dispersible only in water when they contain Cl<sup>-</sup> or Br<sup>-</sup> counter ions. Further studies indicates that fluorine-based anions such as BF<sub>4</sub><sup>-</sup>, PF<sub>6</sub><sup>-</sup>, and Tf<sub>2</sub>N<sup>-</sup> permit the dispersion of imidazolium-modified CNTs only in organic solvents (CHCl<sub>3</sub>), forming black homogeneous solutions. In their study, Chaban and Prezhdo [23] suggested that highly viscous liquid composed of asymmetrical cations and small anions can penetrate inside the apolar CNTs at ambient pressure and high temperatures. Recently, Taherkhani and Minofar [24] studied the effect of impurity and radius of CNT on glass transition and electrical conductivity of 1-ethyl-3-methylimidazolium hexafluorophosphate [EMIM][PF<sub>6</sub>]

encapsulated in CNT, using molecular dynamic simulations (MDS). Their study discovered that the electrical conductivity of [EMIM][PF<sub>6</sub>]/CNT increases with increasing radius of CNT, whereas the electrical conductivity of [EMIM][PF<sub>6</sub>] decreases significantly when encapsulated in zigzag CNT. Chen *et al.*, [25] reported the encapsulation of 1-butyl-3-methylimidazolium hexafluorophosphate in MWCNTs, and they observed that ILs coated in the hollow interior of MWCNTs produces ILs/MWCNT composites with high thermal stability due to the presence of *van der Waals* and H-bonding interactions. Ohba *et al.*, [26] reported that cations adhere weakly to the sidewalls of CNTs, while anions move freely inside the interior of CNTs.

Studies on the mechanisms of interactions between carbon nanotubes (CNTs) and ionic liquids suggested that ILs interact with CNTs via  $\pi$ -cation and/or  $\pi$ - $\pi$  interactions [25, 27-28]. In other studies, weak *van der Waals* or electrostatic forces inferred as basic interactions behind the formation of CNTs-ILs composites [29-31]. For instance, Fileti and Chaban [32] conducted a study where they concluded that fullerene-ionic liquid binding forces were not exclusively of the *van der Waals* interactions. In this study, we report the synthesis and surface functionalization of MWCNTs with some new hydrophobic and hydrophilic ionic liquids (ILs). The ILs-MWCNT composites were studied by spectroscopic techniques, electron microscopy (SEM), and thermal studies. The solubility and dispersibility of MWCNTs were also investigated.

## 2. Experimental

### 2.1 Reagents

All chemicals were obtained from Sigma-Aldrich and BDH chemicals Ltd, and were used as received without further purification unless stated otherwise. Graphite powder ( $< \mu\text{m}$ , synthetic, Switzerland), sulphuric acid (95-99%, A.R), nitric acid (70%, A.R), sodium nitrate ( $>98\%$ , ex  $\text{NO}_3$ ), dimethyl sulfoxide (ACS,  $\geq 99.9\%$  for analysis), dichloromethane (ACS reagent, ISO,  $\geq 99.9\%$ , GC), acetonitrile ( $\geq 99.9\%$ , gradient analysis), methanol (ACS, ISO, reagent, Ph Eur for analysis), ethanol ( $\geq 99.5\%$ , A.R), potassium hexafluorophosphate ( $\geq 99\%$ , solid), bromopropane (99%), 2-bromopropane (99%), pyridine (ACS reagent,  $\geq 99.0\%$ ), and 1-methylimidazole ( $\geq 99\%$ , purified by redistillation).

### 2.2 Synthesis of carbon nanotubes (CNTs)

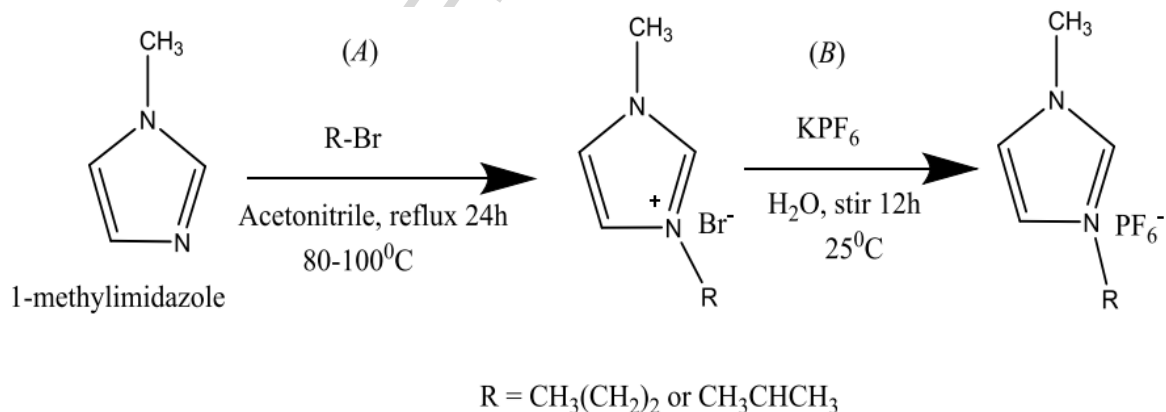
Carbon nanotubes were synthesized using a simple chemical method according to Leo and Seo [33]. Solution of graphite powder (5 g) in water (5 mL), and solution of nitric acid (25 mL) and sulphuric acid (50 mL) were prepared separately at low temperature (ice-bath) under constant stirring. The two solutions were mixed followed by the addition of sodium nitrate (25 g) at  $0^\circ\text{C}$ . The mixture was stirred for 36h at ambient temperature, and further refluxed

for 12h at 90°C. Thereafter, the mixture was centrifuged, neutralized with sodium hydroxide solution, and filtered to obtain the CNTs.

### 2.3 Synthesis of MWCNTs

MWCNTs were synthesized from as-synthesized CNTs, where 0.317g of CNTs was ultrasonicated for 5 minutes in a mixture of concentrated sulphuric acid (15 mL H<sub>2</sub>SO<sub>4</sub>, 65%)/5 mL nitric acid (HNO<sub>3</sub>, 98%), 3:1 by volume. The solution was refluxed for 5h at 60°C, and then washed with distilled water to neutralize acid residue, dried in air vacuum at 70°C to obtain the MWCNTs.

### 2.4 Synthesis of imidazolium-based ILs [3]



**Scheme 1** Synthetic route of imidazolium-based ILs.

**2.4.1 3-methyl-1-propylimidazolium bromide [MPlm<sup>+</sup>][Br<sup>-</sup>]**(Scheme 1A): Into a two-neck round bottom flask fitted with reflux condenser, 5 mL of 1-methylimidazole, 2 mL of 1-bromopropane in 10 mL of acetonitrile were added. The mixture was refluxed for 12 hours at 80-100°C with stirring until the formation of two organic phases. The top layer which contained unreacted materials was discarded, and the colourless viscous lower layer was dissolved in two portions of 20 mL dichloromethane. Thereafter, the solvents were removed under vacuum. Colourless viscous liquid was obtained and dried in an oven at 70°C.

**<sup>1</sup>H NMR (400 MHz, ppm, DMSO-*d*<sup>6</sup>, δ):** 7.185 (1H, s, Im-H<sub>f</sub>), 7.061 (1H, s, Im-H<sub>g</sub>), 4.239-4.204 (2H<sub>c</sub>, t, CH<sub>2</sub>), 3.963 (3H<sub>d</sub>, s, CH<sub>3</sub>), 3.775 (1H, s, Im-H<sub>e</sub>), 1.992-1.902 (2H<sub>b</sub>, m, CH<sub>2</sub>), 0.999-0.962 (3H<sub>a</sub>, t, CH<sub>3</sub>). **<sup>13</sup>C NMR (400 MHz, ppm, D<sub>2</sub>O-*d*<sup>6</sup>, δ):** 10.05 (C1), 22.94 (C2), 39.00 (C5), 51.34 (C3), 122.26 (C4), 123.55 (C7), 127.56 (C6).

**FT-IR (ν/cm<sup>-1</sup>):** 3289-3110 (=C-H, & C-H<sub>sp</sub><sup>2</sup>, m), 2854 (C-H<sub>sp</sub><sup>3</sup>, m), 1648 (C=C, m), 1132 & 989 (C-N, s).

**2.4.2 1-isopropyl-3-methylimidazolium bromide [IsopropylMIm<sup>+</sup>][Br<sup>-</sup>]**(Scheme 1A): Into a two-neck round bottom flask fitted with reflux condenser, 5 mL of 1-methylimidazole, 2 mL of 2-bromopropane in 10 mL of acetonitrile were added. The mixture was refluxed for 12 hours at 80-100°C while stirring until the formation of two organic phases. The top layer which contained unreacted materials was discarded, and the golden viscous lower layer was

dissolved in two portions of 20 mL dichloromethane. Thereafter, the solvents were removed by vacuum. Golden viscous oily liquid was obtained and dried in an oven at 70°C.

**<sup>1</sup>H NMR (400 MHz, ppm, DMSO-*d*<sup>6</sup>, δ):** 9.4798 (1H, s, Im-H), 7.9426-7.6867 (2H, t, 2Im-H), 4.3490-4.3131 (2H, t, CH<sub>2</sub>), 4.0512 (3H, s, CH<sub>3</sub>), 1.9333-1.8787 (2H, m, CH<sub>2</sub>), 0.9101-0.8731 (3H, t, CH<sub>3</sub>). **<sup>13</sup>C NMR (400 MHz, ppm, D<sub>2</sub>O-*d*<sup>6</sup>, δ):** 22.06 (C1, 2), 33.32 (C5), 35.92 (C3), 52.98 (C4), 123.46 (C7), 127.55 (C6).

**FT-IR (ν/cm<sup>-1</sup>):** 3391-3150 (=C-H, & C-H<sub>sp</sub><sup>2</sup>), 2891 (C-H<sub>sp</sub><sup>3</sup>, m), 1561 (C=C, s), 1101-998 (C-N,s).

#### 2.4.3 *1-isopropyl-3-methylimidazolium hexafluorophosphate [IsopropylMIm<sup>+</sup>][PF<sub>6</sub><sup>-</sup>]*

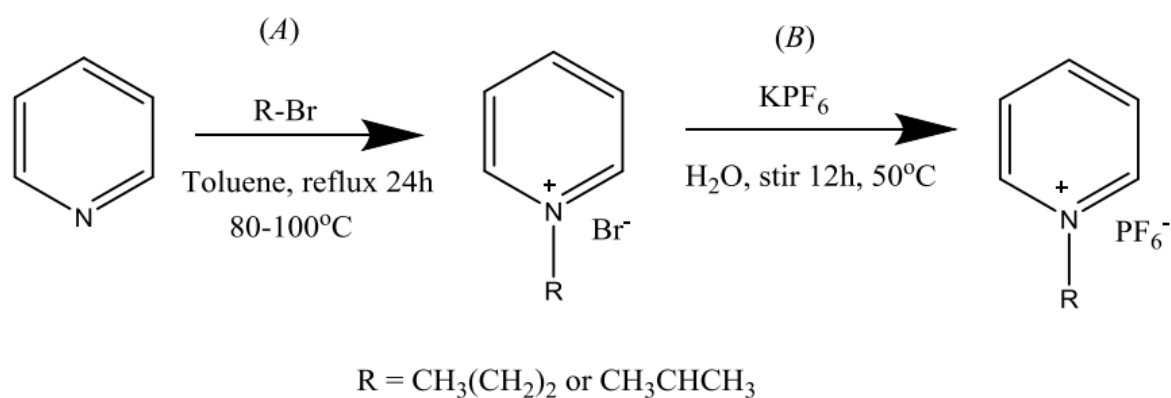
(Scheme 1B): 3.0 mL of [IsopropylMIm<sup>+</sup>][Br<sup>-</sup>] and 3.0 g of potassium hexafluorophosphate were mixed in a 50 mL round bottom flask with 10 mL of water. The reaction mixture was stirred for 12 hours at room temperature. Then the resultant product was rinsed with several portions of water and dissolved in 20 mL dichloromethane, and dried in anhydrous magnesium sulphate (MgSO<sub>4</sub>). The solvent was then removed by vacuum. The resultant golden liquid was dried for 12 hours under vacuum at 70°C.

**<sup>1</sup>H NMR (400 MHz, ppm, DMSO-*d*<sup>6</sup>, δ):** 9.1536 (1H, s, Im-H), 7.8594-7.8603 (1H, t, Im-H), 7.7003-7.6916 (1H, t, Im-H), 4.6473-4.58603 (1H, m, CH), 3.8344 (3H, s, CH<sub>3</sub>), 1.4761-1.4554 (6H, d, CH<sub>3</sub>X<sub>2</sub>). **<sup>13</sup>C NMR (400 MHz, ppm, DMSO-*d*<sup>6</sup>, δ):** 22.79 (C1, 2), 36.19 (C5), 40.04 (C3), 52.62 (C4), 120.92 (C7), 124.15 (C6).

$^{31}\text{P}$  NMR (DMSO- $d^6$ ,  $\delta$ ): -130.94 to -159.12 ppm (m,  $\text{PF}_6^-$ ,  $^1J_{\text{p-f}} = 715.09$  Hz).  $^{19}\text{F}$  NMR (DMSO- $d^6$ ,  $\delta$ ): -69.35 to -71.01 ppm (d,  $\text{PF}_6^-$ ).

FT-IR ( $\nu/\text{cm}^{-1}$ ): 3361 (=C-H, m), 3091 (C-H $_{\text{sp}^2}$ , s), 2872 (C-H $_{\text{sp}^3}$ , m), 1591 (C=C, m), 1150-1110 (C-N, s).

### 2.5 Synthesis of pyridinium-based ILs [3]



**Scheme 2** Synthetic route for pyridinium-based ILs.

**2.5.1 N-propyl pyridinium bromide** [*N*-propylPyr $^+$ ][Br $^-$ ](Scheme 2A): Into a vigorously stirred solution of pyridine (4.21 mL, 52.10 mmol) and 20 mL Toluene at 0°C, 1-bromopropane (4.09 mL, 45.0 mmol) was added slowly in three-neck flask. The mixture was heated to reflux at 100°C for 24 hours. Toluene was decanted and the remaining brown to gold viscous liquid was re-crystallized in dichloromethane twice. Dichloromethane was removed under vacuum and the product was dried in an oven at 70°C for 10 hours to further

remove any solvent residue. The product obtained was *N*-propyl pyridinium bromide [*N*-propylPyr]<sup>+</sup>[Br].

**<sup>1</sup>H NMR** (400 MHz, ppm, DMSO-*d*<sup>6</sup>,  $\delta$ ): 9.27-9.26 (2H, d, pyr-CH<sub>o</sub>), 8.19-8.16 (2H, t, pyr-CH<sub>m</sub>), 8.66-8.62 (1H, t, pyr-CH<sub>p</sub>), 4.69-4.66 (2H, d, CH<sub>2</sub>), 1.95-1.87 (2H, m, CH<sub>2</sub>), 0.83-0.78 (3H, t, CH<sub>3</sub>).

**FT-IR** (ν/cm<sup>-1</sup>): 3348 (=C-H, w), 2870 (C-H<sub>sp<sup>3</sup></sub>, s), 1591 (C=C<sub>pyr</sub>, s), 1417 (C=N<sub>pyr</sub>, m), 1145 (C-N, m).

### 2.5.2 *N*-isopropyl pyridinium hexafluorophosphate [*N*-isopropylPyr]<sup>+</sup>[PF<sub>6</sub><sup>-</sup>](Scheme 2B):

Viscous liquid of [*N*-isopropylPyr]<sup>+</sup>[Br]<sup>-</sup> (1.0 mL), and 2.02 g (11 mmol) of potassium hexafluorophosphate salt were mixed in a 100 mL round bottom flask containing 10 mL of water and stirred for 12 hours at 50°C. The resultant product was re-crystallized from dichloromethane (2 x 10 mL) and dried with anhydrous magnesium sulphate to remove water residue. The solvent was evaporated by vacuum rotary evaporator at 40°C. Light brown to gold solid products were obtained and further dried at 70°C for 2 hours in an oven. It was observed that the products melt and become liquids in an oven, while it tends to crystallize in fume hood at room temperature.

**<sup>1</sup>H NMR** (400 MHz, ppm, DMSO-*d*<sup>6</sup>,  $\delta$ ): 9.17- 9.15 (2H, d, pyr-CH<sub>o</sub>), 8.61 -8.57 (1H, m, pyr-CH<sub>p</sub>), 8.17- 8.13 (2H, t, pyr-CH<sub>m</sub>), 5.03- 5.01 (1H, m, CH), 1.62 – 1.61 (6H, d, CH<sub>3</sub>x2).

**<sup>31</sup>P NMR** (DMSO-*d*<sup>6</sup>,  $\delta$ ): -131.54 to -157.32 ppm (m, PF<sub>6</sub><sup>-</sup>, <sup>1</sup>J<sub>p-f</sub> = 713.09 Hz). **<sup>19</sup>F NMR** (DMSO-*d*<sup>6</sup>,  $\delta$ ): -69.25 to -71.13 ppm (d, PF<sub>6</sub><sup>-</sup>).

**FT-IR** (ν/cm<sup>-1</sup>): 3336 (=C-H<sub>pyr</sub>, m), 3150-3109 (C-H<sub>sp<sup>2</sup></sub>, m), 2907 (C-H<sub>sp<sup>3</sup></sub>, m), 1635 (C=C<sub>pyr</sub>, s), 1486 (C=N<sub>pyr</sub>, s), 1156 (C-N).

## 2.6 Synthesis of ILs-MWCNT composites

ILs-MWCNT composites were synthesized according using reported methods with minor modifications [17, 25, 34]. Briefly, a solution of 5 mg of MWCNTs and 10 mg of each ILs in 10 mL of *N,N*-dimethylformamide (DMF) was ultrasonicated for 20 mins. The mixture was then vigorously stirred for 24h at 50°C. The unreacted MWCNTs residues were removed by centrifugation. Thereafter, ILs-MWCNT composites were filtered, thoroughly washed with DMF, ethanol, and water, respectively.

## 2.7 Characterization techniques

Fourier transform infrared spectroscopic measurements were carried out using Perkin- Elmer, Universal ATR sampling Accessory.  $^1\text{H}$ ,  $^{13}\text{C}$ ,  $^{31}\text{P}$ , and  $^{19}\text{F}$ -nuclear magnetic resonance (NMR) spectra were obtained in  $\text{D}_2\text{O}$  and  $\text{DMSO}-d^6$  on a Bruker Avance III 400 at frequencies 500 MHz or 400 MHz ( $^1\text{H}$ ). Thermal stability of MWCNTs, ILs, and ILs-functionalized composites were determined by Perkin-Elmer TGA 4000 using 10-30mg of sample heated in the temperature range of 50-900°C at a heating rate of 40°C/min under nitrogen flow. Scanning electron microscopy (SEM) micrographs were taken using Zeiss Evols 15 Scanning electron microscopy combined with energy dispersive X-ray spectroscopy (EDXS).

### 3. Results and Discussion

#### 3.1 Nuclear magnetic resonance studies

The  $^1\text{H}$ -NMR spectra of imidazolium-based ionic liquids showed large frequency downshift and overlapping of three proton peaks around the imidazole ring. For instance, the protons in positions 4 and 5 were found to resonate or de-shielded (downfield signal) around low field due to the presence of bromide ions for halide-containing ILs shows the proton NMR of [*N*-propylPyr] $^+$ [Br] $^-$ , and [*N*-isopropylPyr] $^+$ [PF $_6$ ] $^-$ . As it is observed, the signals between 9.162-8.147 ppm corresponds to the pyridinium ring protons at *ortho*-, *meta*-, and *para*-positions. For [*N*-propylPyr] $^+$ [Br] $^-$  on the hand, the triplet, multiplet, and triplet due to the  $-\text{CH}_2$  attached to the pyridyl nitrogen,  $-\text{CH}_2$  and  $-\text{CH}_3$  of propyl moiety can be observed around upfield region, respectively. Proton NMR for [*N*-isopropylPyr] $^+$ [PF $_6$ ] $^-$  further shows multiplet around 5.051-4.984 ppm corresponding to the single proton of the central carbon of the isopropyl group, and a doublet around 1.625-1.609 ppm corresponding to the six protons of ( $-\text{CH}_3 \times 2$ ) of the isopropyl group. The  $^{13}\text{C}$ -NMR spectra of the ILs showed direct information about the carbon skeleton and the number of equivalents/non-equivalents carbons of the ILs. Generally, the presence of electronegative atoms and  $\pi$ -bonds causes downfield chemical shifts. For example, C4, C6, and C7 of the imidazolium rings are deshielded (shifted downfield) due to the presence of the  $\pi$ -electron system in the imidazolium ring and the

influence of the attached electronegative bromide counter-ion. As expected, C1 and C2 of all isopropyl-containing ILs are chemically equivalent and are assigned to one signal. However, the appearance of the peak at 40.041 ppm corresponds to the overlap of the C3 carbon of the isopropyl group and the DMSO solvent.  $^{31}\text{P}$  NMR spectra of both hydrophobic ILs were found to have multiplet (m) between -130 to -159 ppm confirming the presence of the phosphorous atom coupled with six fluorine atoms. On the other hand, the  $^{19}\text{F}$  NMR spectra were found to contain doublets (d) between -69 to -71.0 ppm that confirmed the coupling of six fluorine atoms with one phosphorous atom. To further complement the,  $^1\text{H}$ ,  $^{13}\text{C}$ ,  $^{19}\text{F}$ , and  $^{31}\text{P}$ -NMR results, single mass analysis data of the synthesized compounds based on C, H, and N established that the experimental accurate mass values (125.1075, 122.0966, and 122.0973 m/z for methyl-propyl imidazolium, isopropyl-methyl imidazolium, isopropyl pyridinium and propyl pyridinium, respectively) are in agreement with their calculated mass from respective molecular formulas. This thus confirmed synthesis of the compounds [3].

### 3.2 Infrared spectral studies

FTIR spectra of MWCNTs and ILs-MWCNT composites provide information about the functional groups present in the MWCNTs with ILs. Figs. 1 & 2 shows the FTIR spectra of pure ILs (Fig. 1), and FTIR spectra of MWCNTs and ILs-modified MWCNT hybrids (Fig. 2). As shown in Fig. 1, the FTIR spectrum of  $[N\text{-propylPyr}^+][\text{Br}^-]$  shows a very weak band at

3348  $\text{cm}^{-1}$  which can be attributed to  $=\text{C}-\text{H}$  stretch in *ortho*, *meta*, and *para* positions of the pyridinium cation. The strong stretching vibrations found at 2870 and 1579  $\text{cm}^{-1}$  are ascribed to  $\text{C}-\text{H}_{\text{sp}^3}$  of propyl group, and  $\text{C}=\text{C}$  of pyridine, respectively. Weak to medium peaks observed at 1417 and 1145  $\text{cm}^{-1}$  are due to  $\text{C}=\text{N}$  of pyridinium cation, and  $\text{C}-\text{N}$  between the nitrogen of pyridinium ring and first carbon of propyl, respectively.

The FTIR spectrum of [*N*-isopropylPyr<sup>+</sup>][PF<sub>6</sub><sup>-</sup>] appeared similar but less shifted vibrational bands compared to bromide containing ILs-counterparts. Another important peak found around 2976  $\text{cm}^{-1}$  assigned to  $\text{C}-\text{H}_{\text{sp}^3}$  of the isopropyl group attached to pyridinium cation. [M<sup>+</sup>Im<sup>+</sup>][Br<sup>-</sup>] FTIR spectrum shows well pronounced peaks in the range 3390-3150  $\text{cm}^{-1}$  assigned to the  $=\text{C}-\text{H}$  stretch and  $\text{C}-\text{H}_{\text{sp}^2}$  stretching vibrations. The shifts in the peaks could be attributed to the presence of halide counter ions. The peaks at 2891 and 1561  $\text{cm}^{-1}$  are assigned to the  $\text{C}-\text{H}_{\text{sp}^3}$  of propyl and  $\text{C}=\text{C}$  of the imidazolium ring, respectively. The strong vibrational bands in the range 1101-998  $\text{cm}^{-1}$  were ascribed to the presence of the  $\text{C}-\text{N}$  functional group between the imidazolium ring and alkyl groups. The FTIR spectrum of [*N*-isopropylMIm<sup>+</sup>][PF<sub>6</sub><sup>-</sup>] shows similar vibrational bands compared to that of [M<sup>+</sup>Im<sup>+</sup>][Br<sup>-</sup>] but shifted slightly. Stretching vibrations of  $\text{C}-\text{H}_{\text{sp}^3}$  of propyl and isopropyl were observed in relatively similar position [25].

As shown in Fig. 2, the FTIR spectrum of MWCNTs shows stretching vibrations at  $1734\text{ cm}^{-1}$  corresponding to the carboxylic and graphite groups on the surface of pure nanotubes. A weak OH stretching vibration around  $3598\text{ cm}^{-1}$  is due to the moisture content absorbed by the carbon materials and was also confirmed by the thermogravimetric analysis [26, 34]. Other important vibrational bands found at  $2323$  and  $1239\text{ cm}^{-1}$  are attributed to  $\text{CO}_2$ , and C-O, respectively. After functionalization, the skeletal vibrational bands of graphitic and carboxylic groups at  $1734\text{ cm}^{-1}$  corresponding to C=O disappeared in ILs-MWCNT composites spectral. The shift of the weak OH stretching vibration from  $3619\text{ cm}^{-1}$  to  $3789\text{ cm}^{-1}$  in the ILs-MWCNT composites with bromide ions indicates successful modification. The sharp peak at  $3170\text{ cm}^{-1}$  is ascribed to the stretching vibration of C-H<sub>sp</sub><sup>2</sup> of the ILs heterocyclic rings in the ILs-MWCNTs composites. The introduction of ionic liquids on the surface of the nanotubes does change the functional groups or morphology of the nanotubes. It can also be stated that the disappearance or less intense of former pure ILs stretching vibration bands signify the total incorporation of ILs with carbon nanotubes and the formation of new functional composites with completely different properties. The vibrational bands around  $798$  and  $788\text{ cm}^{-1}$  are ascribed to P-F bond stretching in hydrophobic ILs. The results obtained from the FTIR spectra studies indicates that the interactions between the ILs with MWCNTs occur via non-covalent interactions after functionalization.

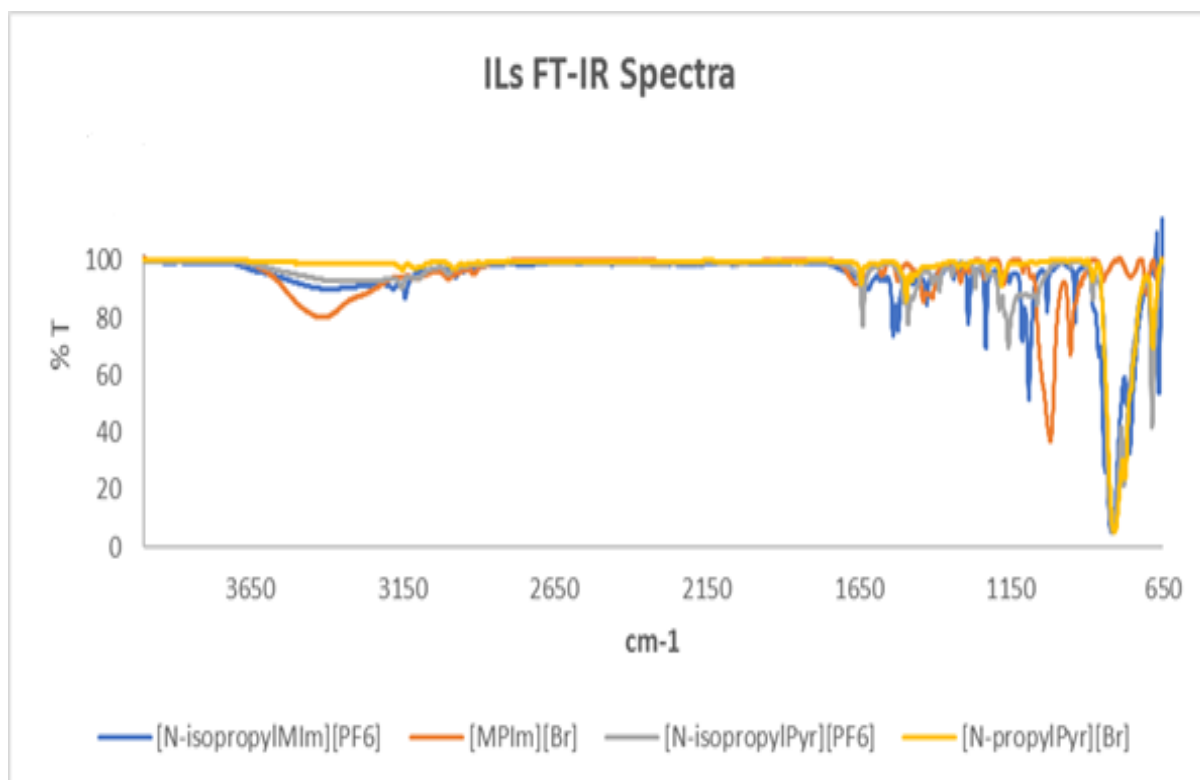
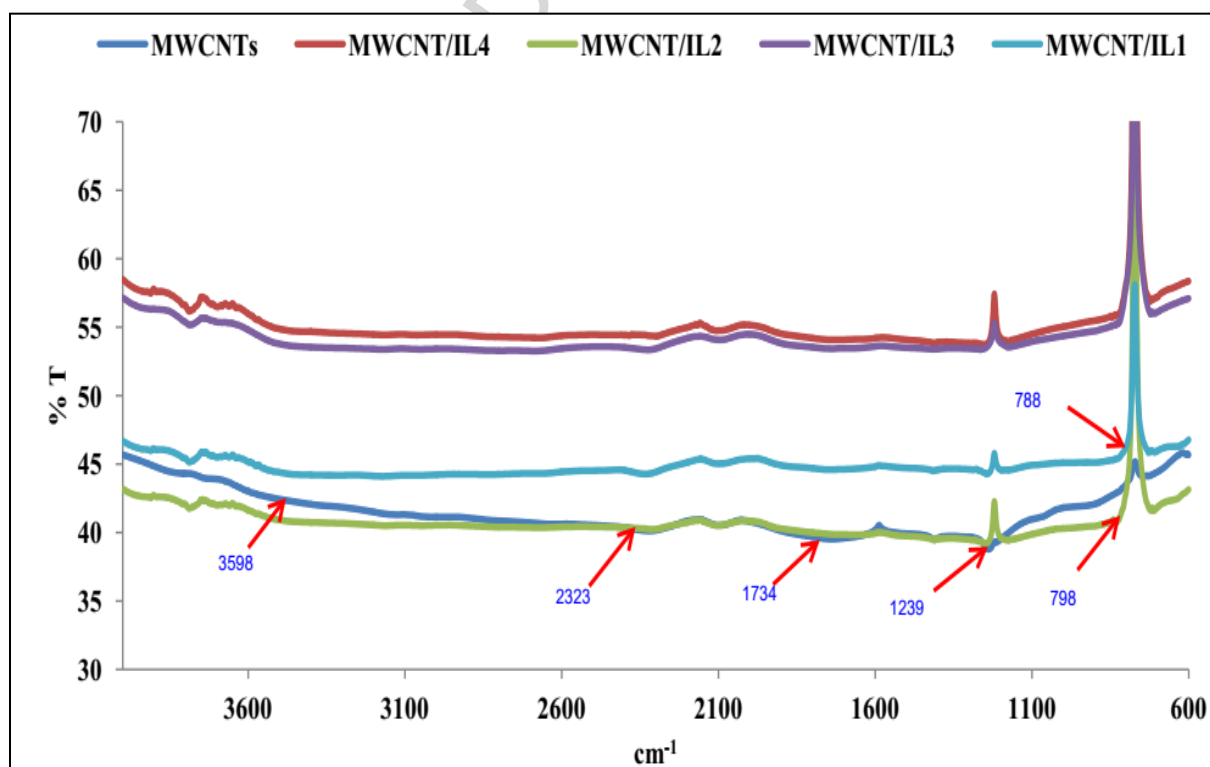


Figure 1 FTIR spectra of ILs.



**Figure 2** FTIR spectra of MWCNTs and IL-MWCNT composites, IL1= [IsopMIm][PF<sub>6</sub>], IL2= [N-IsopPyr][PF<sub>6</sub>], IL3= [MPIIm][Br], IL4= [N-PropylPyr][Br].

### 3.3 Thermogravimetric analysis of ILs and ILs-MWCNT composites

Thermogravimetric analysis (TGA) was used to gather information about the thermal degradation of ILs and ILs-MWCNT composites synthesized. TGA results obtained for functionalized materials were compared with those of pure ILs and MWCNTs, respectively. As shown in Fig. 3, the ILs exhibit weight loss at different temperatures. The [MPIIm<sup>+</sup>][Br<sup>-</sup>] showed a weight loss of  $T_d$ , < 30% with onset decomposition at 250°C and complete second decomposition around 400 °C. Another imidazolium-based ILs, [isopropylMIm<sup>+</sup>][PF<sub>6</sub><sup>-</sup>] shows a considerable stability with weight degradation recorded to be less than 15% at 400 °C. However, at 450 °C, a complete decomposition of [isopropylMIm<sup>+</sup>][PF<sub>6</sub><sup>-</sup>] ILs was observed.

In the thermal analysis of the pyridinium-based ILs, [N-propylPyr<sup>+</sup>][Br<sup>-</sup>] weight decreased steadily with increasing temperature and reached 99% weight loss around 350°C, whereas [N-isopropylPyr<sup>+</sup>][PF<sub>6</sub><sup>-</sup>] showed multi-step degradation profile with highest thermal stability up to 400°C and less than 35% weight loss was recorded above 450 °C. It was also observed that hydrophobic ILs exhibits high thermal stability than their hydrophilic counterparts and both of them were thermally stable up to 400 °C.

Fig. 4 shows the thermograms of MWCNTs and ILs-MWCNT composites. Pure MWCNTs thermogram showed multi-steps degradations, though the weight loss is insignificant (initial step at  $T_d$ , 5% around 250°C, and final degradation step at  $T_d$ , 10% around 750°C). The TGA results obtained for the MWCNTs are in agreement with the findings from other studies [35-36]. Comparison of the TGA curves of pure ILs, MWCNTs, and their ILs-functionalized composites clearly shows that ILs-MWCNT composites were highly stable with two major weight losses. The first small weight loss could be attributed to the degradation of ILs on the surface of nanotubes and the second decomposition corresponds to CNTs fragments [37]. It can thus be concluded that composites of ILs-MWCNT are effectively thermally stable than pure ILs and/or MWCNTs [25]. The level of stability of ILs-MWCNT hybrids can be associated with non-covalent (ionic-interactions or exchange), and strong *van der Waals* interactions between the ILs and MWCNTs. Another potential contributing factor to the stability of ILs-MWCNT hybrids could be the differences in polarity of both the dispersing molecule (ILs) and the solute (MWCNTs). However, other studies suggested that the thermal stability of CNT-ILs depends on the type of the ILs counter-ions [37].

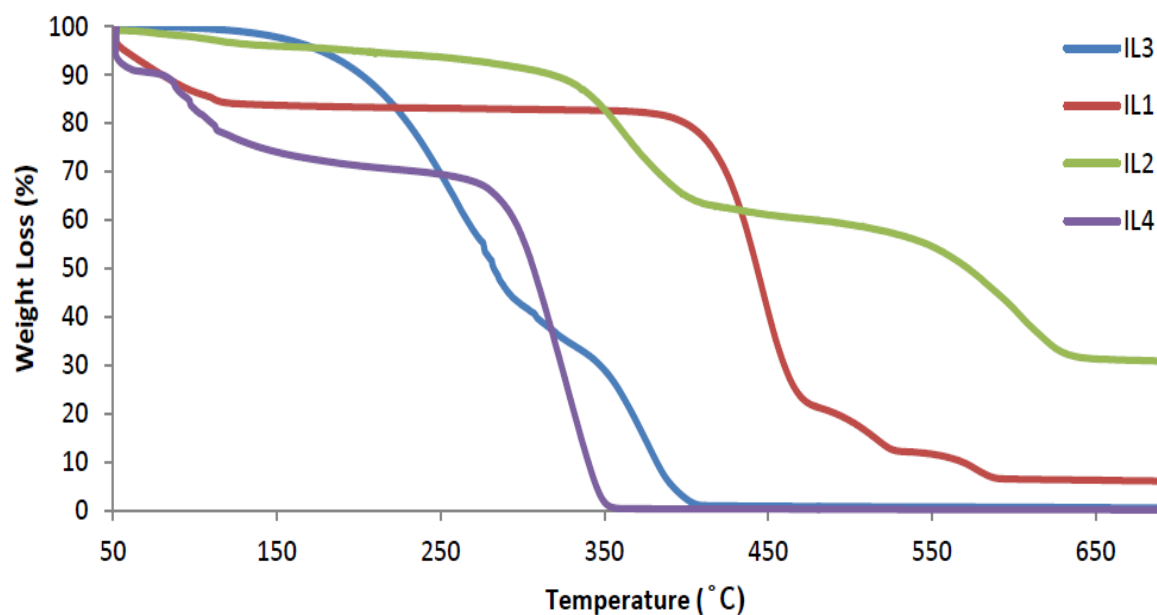


**Figure 3** TGA curves of ILs, IL1= [IsopMIm][PF<sub>6</sub>], IL2= [N-IsopPyr][PF<sub>6</sub>], IL3= [MPIm][Br], IL4= [N-PropylPyr][Br].

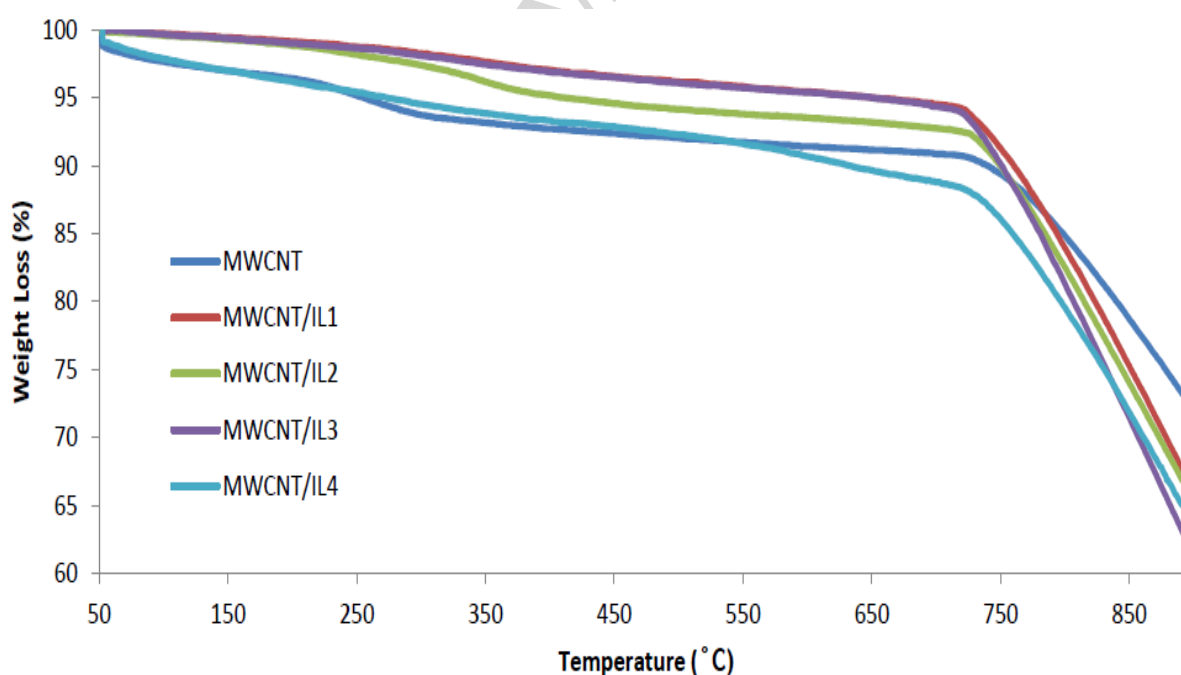


**Figure 4** TGA curves of MWCNTs and IL-MWCNT composites, IL1= [IsopMIm][PF<sub>6</sub>], IL2= [N-IsopPyr][PF<sub>6</sub>], IL3= [MPIm][Br], IL4= [N-PropylPyr][Br].

### 3.4 Solubility studies of the MWCNTs and ILs-MWCNT composites in different solvents

Solubility studies of the MWCNT's and ILs-MWCNT was carried out in nine solvents, polar to non-polar (from left to right) in Figs. 5 & 6: water (H<sub>2</sub>O), ethanol (EtOH), acetonitrile (ACN), dimethyl sulfoxide (DMSO), acetone (Ace), tetrahydrofuran (THF), diethyl ether (DEE), toluene (TOL), and hexane (HEX). Consequently, some MWCNTs and/or their ILs-MWCNT composites were not soluble (N.S), some were partially soluble (P.S), while some were completely soluble (S) in different solvents depending on their polarities. Pure MWCNTs were insoluble or not dispersible in polar solvents such as water and ethanol, yet suspendable in other polar solvents (acetonitrile, dimethyl sulfoxide, acetone, and tetrahydrofuran), (Fig. 5). On the other hand, MWCNTs were insoluble in non-polar solvents (diethyl ether, toluene, and hexane). As it was once suggested by Salam & Burk [20], a solvent or solute will only dissolve or be dissolved in a substance of similar polarity, respectively. Therefore, the latter solubility characteristics of MWCNTs can be attributed to its hydrophobicity character (non-polar substance). Another important observation is the relative insolubility of MWCNTs in more non-polar solvents such as toluene and hexane. This indicates that differences in polarity between MWCNTs and other non-polar solvents played a significant role.

The solubility of different ILs-MWCNT hybrids in different solvents is presented in Fig. 6. Fig. 6(A) shows the solubility of  $[N\text{-isopropylPyr}^+][\text{PF}_6^-]/\text{MWCNT}$  which indicates the composite is insoluble in all solvents. On the other hand, the composite of MWCNTs with hydrophilic pyridinium-based ILs such as  $[N\text{-propylPyr}^+][\text{Br}^-]/\text{MWCNT}$  provided different solubility trends. As shown in Fig. 6(D),  $[N\text{-propylPyr}^+][\text{Br}^-]/\text{MWCNT}$  showed varied solubility profiles by being insoluble and slightly soluble in polar solvents with varied polarity index, while it showed better solubility in most non-polar solvents. This suggests non-polar and hydrophobicity character of the solute were maintained after functionalization. Solubility studies of the MWCNT composites with imidazolium-based ILs shown in Fig. 6(B) indicates that the solute was insoluble in water (a strong polar solvent), but soluble in ethanol (another strong polar solvent). Secondly, the same solute was soluble or partially suspended in non-polar solvents except hexane. The insolubility of this composite in water and hexane brings the discussion of polarity level between the solute and the solvent. For instance in this case, strong polar solvent (water) molecules cannot be detached by relatively non-polar substance, and also strong non-polar solvent (hexane) cannot detach MWCNT (non-polar) molecules. This observation is in agreement with the study of Salam and Burk [20].

In the solubility study of  $[\text{isopropylPyr}^+][\text{PF}_6^-]/\text{MWCNT}$  shown in Fig. 6(C), the composite was soluble in hexane and not in water. This latter confirmed the hydrophobicity of the

synthesized material. Based on the solubility study conducted, it can be concluded that when the polarity of both the solvent and the solute are similar, then the solute and the solvent definitely separate each other leading to increase in solubility.

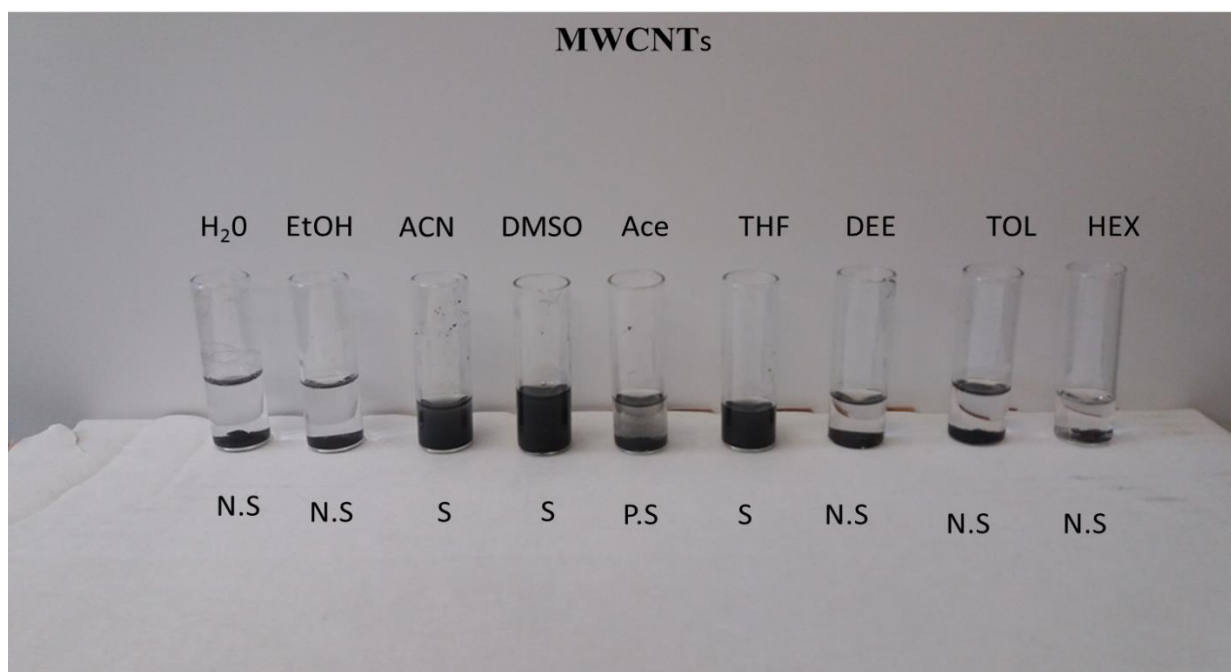


**Figure 5** Solubility of MWCNTs in different solvents.

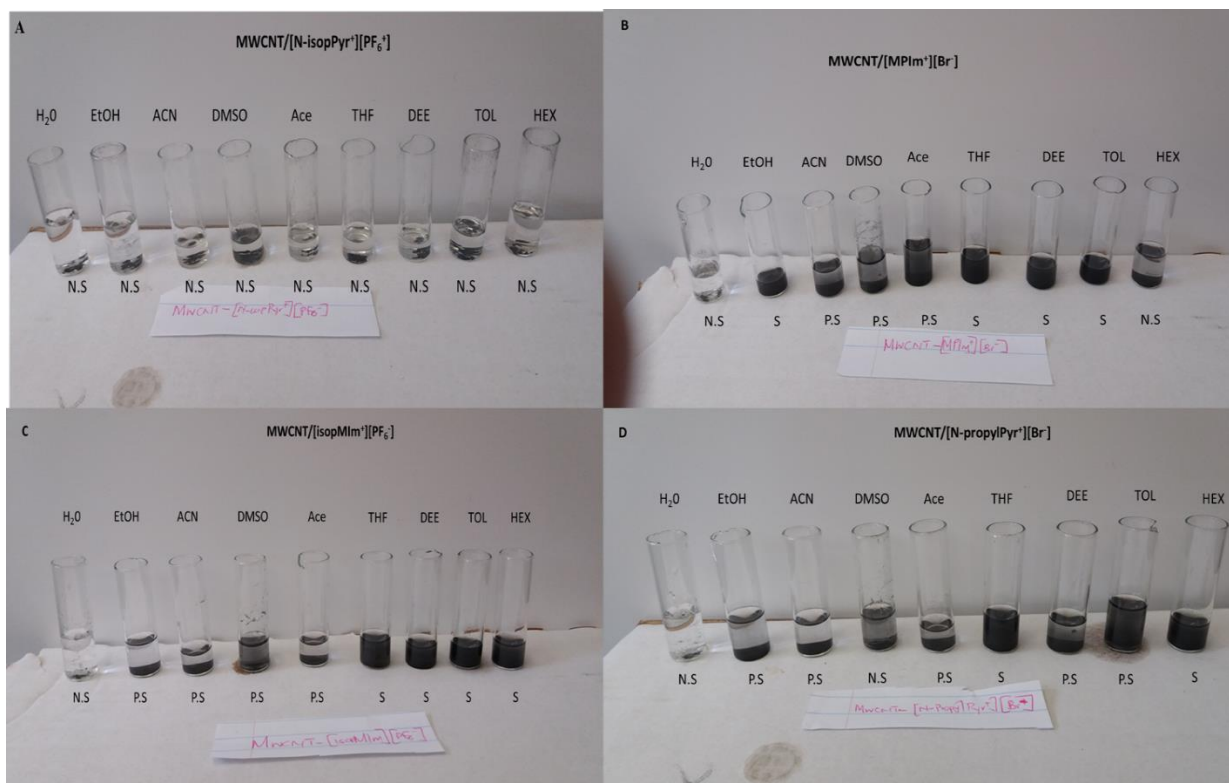


**Figure 6** Solubility of four ILs-MWCNT composites; (A) [N-isopropylPyr<sup>+</sup>][PF<sub>6</sub><sup>-</sup>]/MWCNT, (B) [MPIIm<sup>+</sup>][Br<sup>-</sup>]/MWCNT, (C) [isopropylMIm<sup>+</sup>][PF<sub>6</sub><sup>-</sup>]/ MWCNT, and (D) [N-propylPyr<sup>+</sup>][Br<sup>-</sup>]/MWCNT: Where (S, N.S, and P.S) stands for soluble, non-soluble, and partial soluble, respectively.

### 3.5 Scanning Electron microscopy and EDS spectra of MWCNTs and MWCNT-ILs composites

The surface morphologies of MWCNTs, and the ILs-functionalized hybrids presented in Fig. 7 shows highly twisted or tangled tubes of MWCNTs. Figs. 7 (A) and (B), shows carbon nanotubes with clustered or fused morphologies with limited surface area. The ILs-functionalized MWCNT hybrids shows different morphological orientations. They are well dispersed with uniformly pronounced tubing and increased surface area, while in some areas

the MWCNTS are restacked together inside ionic liquids producing flake-layers orientations [34]. It is also worth noting that the morphology of the MWCNTs is unaltered but shows improved dispersion (Fig. 8). Energy-dispersive X-ray spectroscopy (EDXS) results confirmed the presence of constituents' elements in MWCNTs and ILs-MWCNT composites (Figs. 7 C-D and 9). The intensity of the carbon peak (Fig. 7C-D) shows the amount of carbon material produced [26]. The presence of phosphorous (P) and fluorine in Fig. 9 (A & C) confirms the successfully dispersion of MWCNTs in hydrophobic ILs [25], whereas in Fig. 9 (B & D) the presence of bromide ions signify the combination of halide-containing ILs and MWCNTs.

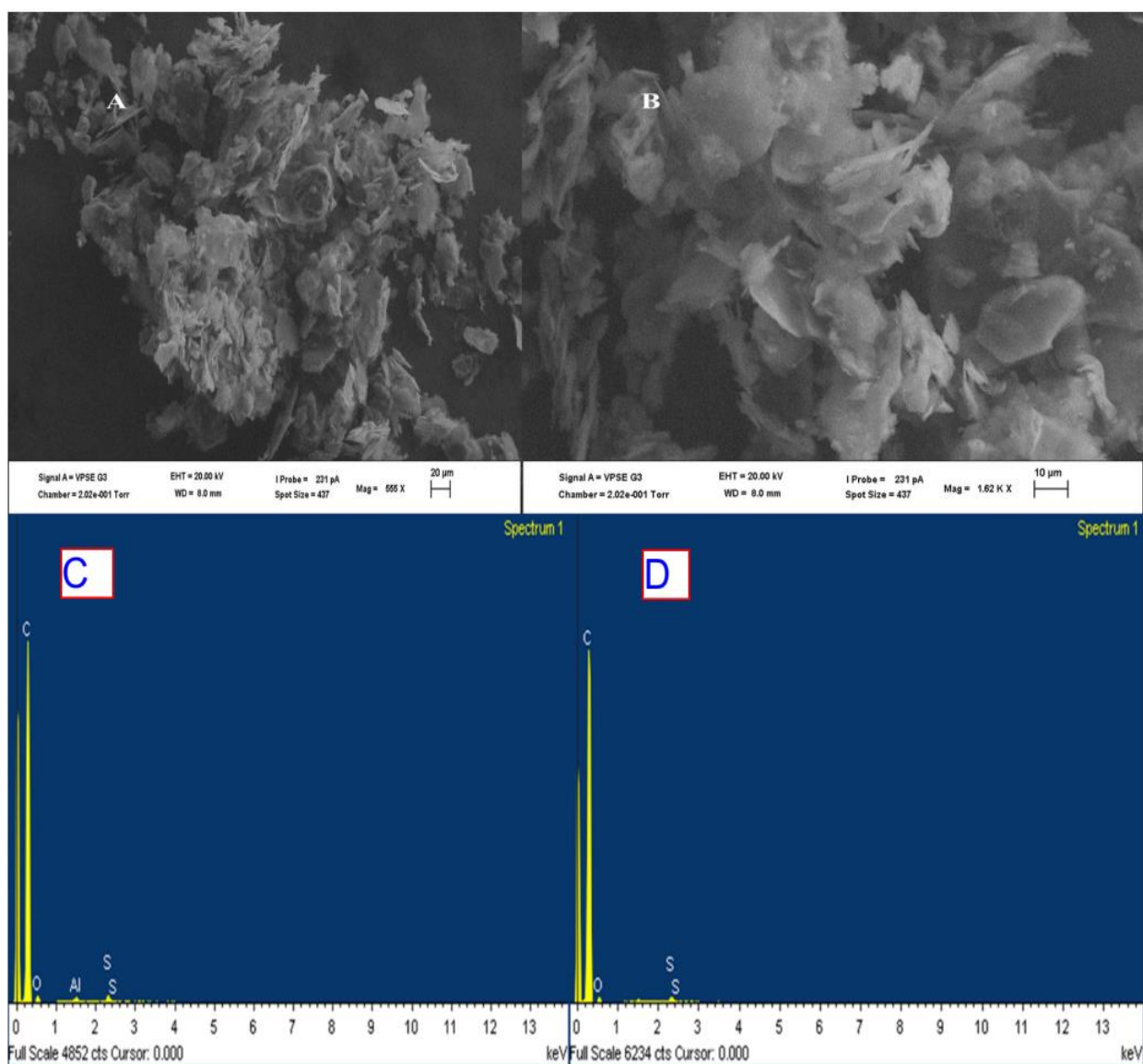


**Figure 7** SEM and EDS spectra of MWCNTs.

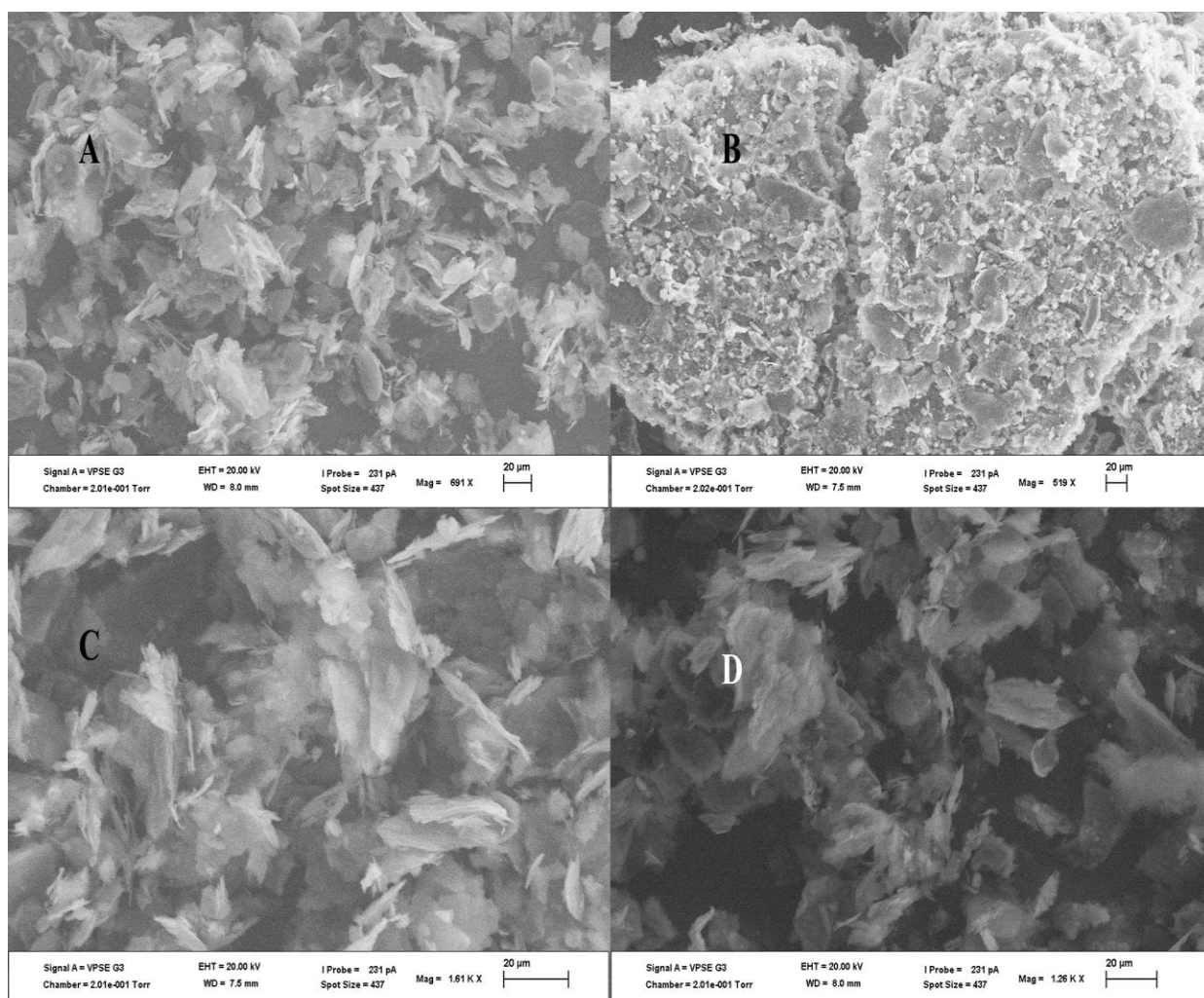


**Figure 8** SEM micrographs of MWCNT-IL composites: (A)  $[N\text{-propylPyr}^+][\text{Br}^-]/\text{MWCNT}$ , (B)  $[N\text{-isopropylPyr}^+][\text{PF}_6^-]/\text{MWCNT}$ , (C)  $[\text{MPIm}^+][\text{Br}^-]/\text{MWCNT}$ , and (D)  $[\text{isopropylMIm}^+][\text{PF}_6^-]/\text{MWCNT}$ .

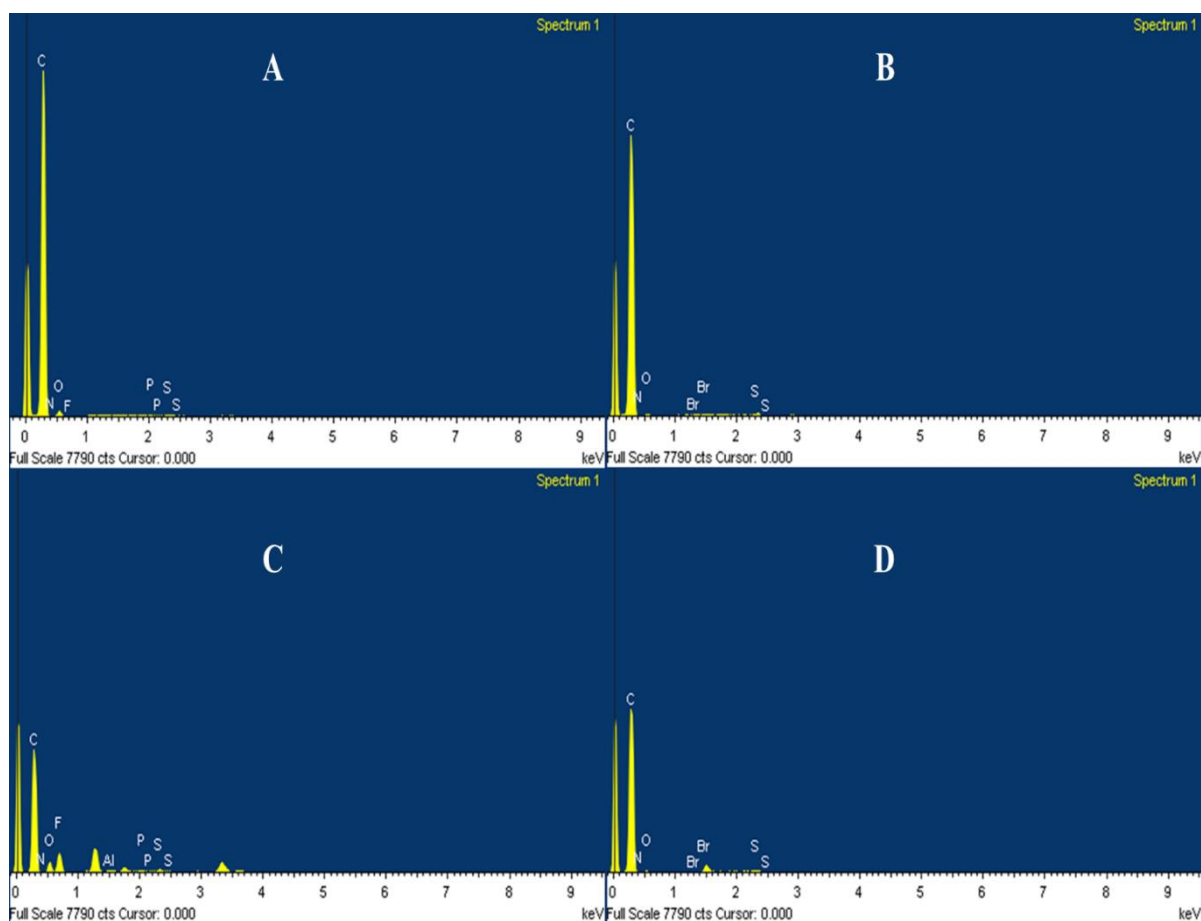


**Figure 9** Elemental content in samples shown from EDS spectra; (A) [isopropylMIm<sup>+</sup>][PF<sub>6</sub><sup>-</sup>]/MWCNT, (B) [MPIIm<sup>+</sup>][Br<sup>-</sup>]/MWCNT, (C) [*N*-isopropylPyr<sup>+</sup>][PF<sub>6</sub><sup>-</sup>]/MWCNT, and (D) [*N*-propylPyr<sup>+</sup>][Br<sup>-</sup>]/MWCNT.

#### 4 Conclusions

MWCNTs, ILs, and ILs-MWCNT composites were synthesised and characterized using FTIR spectroscopy, scanning electron microscopy (SEM), energy dispersive X-ray spectroscopy (EDS), thermogravimetric analysis (TGA), and solubility in different polar and non-polar solvents. NMR spectra studies confirmed the synthesis of the ILs. FTIR spectroscopic studies revealed graphitic and carboxylic functional group in the MWCNTs. Thermal studies shows that the hydrophobic ILs are more thermally stable than hydrophilic counterparts. However, ILs-MWCNT hybrids are also more thermally stable and versatile than individual ILs and/or MWCNT components. The observed high thermal stability in MWCNT composites are ascribed to strong *van der Waals* and non-covalent interactions. Finally, the ILs-MWCNT hybrids were observed to be soluble and/or insoluble in different solvents. The solubility of these composites depends on the polarity of both the solvents and the composites. Therefore, it can be concluded that ILs-MWCNT compounds in this study are hydrophobic (non-polar), immiscible with water and other polar solvents. The as-synthesized thermally stable ILs-MWCNT composites with increased surface area can be used in a number of applications such as metal ions removal (adsorption).

## Acknowledgements

The authors gratefully acknowledge National Research Foundation (NRF) of South Africa and Sasol for financial support. M. Matandabuzo gratefully acknowledges NRF for PhD scholarship.

## References

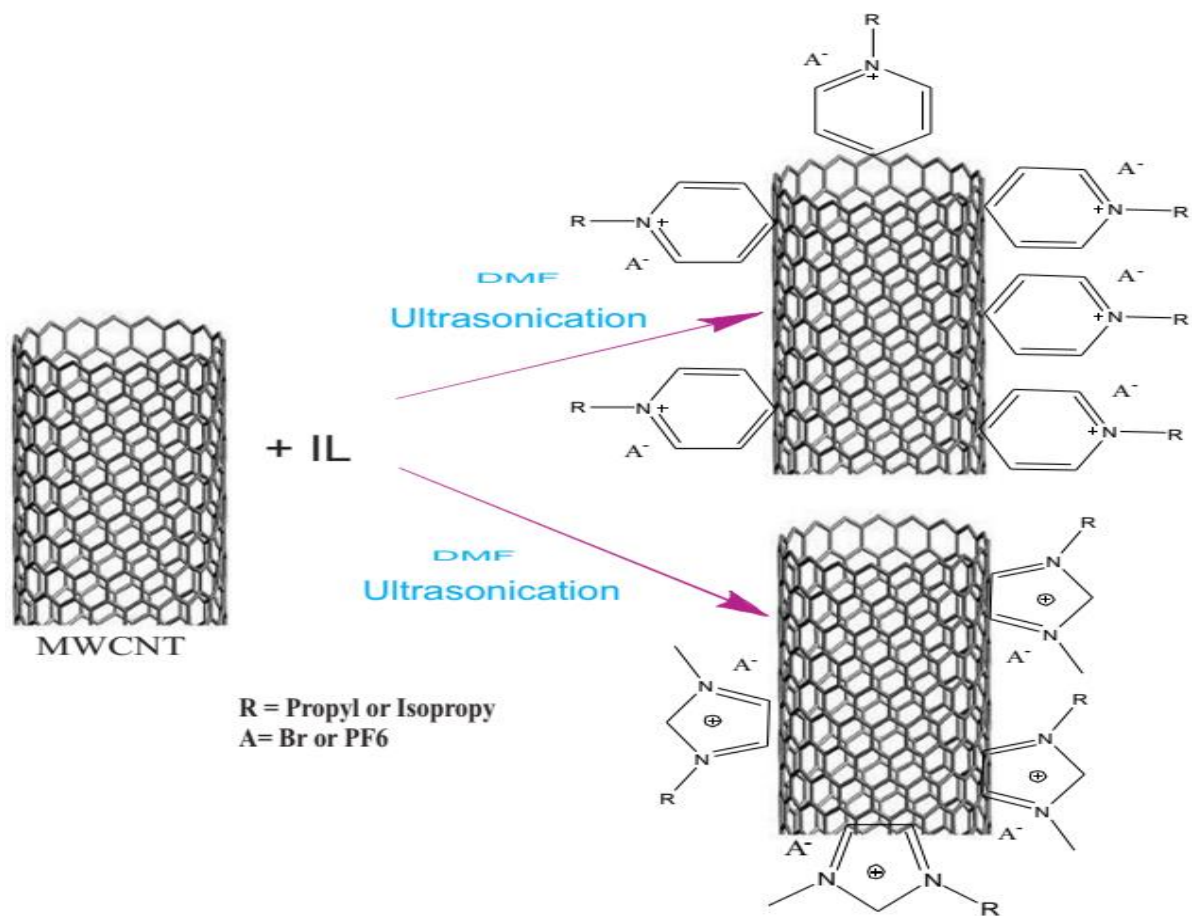
- [1] T. Fukushima, T. Aida, Ionic liquids for soft functional materials with carbon nanotubes, *Chem. Eur. J.* 13 (2007) 5048 – 5058.
- [2] *Ionic Liquids in Synthesis*, edited by P. Wasserscheid and T. Welton, 2nd ed. (Wiley-VCH, Weinheim, 2008).
- [3] M. Matandabuzo, P. A. Ajibade, Synthesis, characterization, and physicochemical properties of hydrophobic pyridinium-based ionic liquids with N-propyl and N-isopropyl, *Z. Anorg. Allg. Chem.* 644 (2018) 489–495.
- [4] N. Terasawa, High-performance ionic and non-ionic fluoropolymer/ionic liquid gel hybrid actuators based on single-walled carbon nanotubes, *RSC Adv.*, 7 (2017) 2443.
- [5] F. Rietzler, J. Nagengast, H.P. Steinrück, F. Maier, Interface of ionic liquids and carbon: Ultrathin [C1C1Im][Tf2N] films on graphite and graphene, DOI:10.1021/acs.jpcc.5b09649.
- [6] J. Dupont, R. F. de Souza, P. A. Z. Suarez, *Chem. Rev.* 102 (2002a) 3667 – 3691; P. Wasserscheid, W. Keim, *Angew. Chem. Int. Ed.* 39 (2000b) 3772 – 3789; *Angew. Chem.* 112 (2000) 3926 – 3945; T. Welton, *Chem. Rev.* 99 (1999d) 2071 – 2083.
- [7] M. Armand, F. Endres, D. R. MacFarlane, H. Ohno, B. Scrosati, *Nat. Mater.* 8 (2009a) 621 – 629; W. Lu, A. G. Fadeev, B. Qi, E. Smela, B. R. Mattes, J. Ding, G. M. Spinks, J. Mazurkiewicz, D. Zhou, G. G. Wallace, D. R. MacFarlane, S. A. Forsyth, M. Forsyth, *Science* 297 (2002b) 983 – 987; c) J. Yuan, M. Antonietti, *Polymer* 52 (2011c) 1469 – 1482; D. Mecerreyes, *Prog. Polym. Sci.* 36 (2011d) 1629 – 1648.
- [8] M. Lazzari, M. Mastragostino, F. Soavi, *Electrochem. Commun.* 9 (2007) 1567–1572.
- [9] L. Zhao, J. Yamaki, M.J. Egashira, M. J., *Power Sources*, 174 (2007) 352–358.
- [10] V. Lockett, R. Sedev, J. Ralston, M. Horne, T.J. Rodopoulos, T. J., *Differential Capacitance of the Electrical Double Layer in Imidazolium-Based Ionic Liquids:*

- Influence of Potential, Cation Size, and Temperature, *Phys. Chem. C* 112 (2008) 7486–7495.
- [11] N. Yamanaka, R. Kawano, W. Kubo, N. Masaki, T. Kitamura, Y. Wada, M. Watanabe, S. Yanagida, Dye-Sensitized TiO<sub>2</sub> Solar Cells Using Imidazolium-Type Ionic Liquid Crystal Systems as Effective Electrolytes, *J. Phys. Chem. B* 111 (2007) 4763-4769.
- [12] J. Zheng, S.S. Moganty, P. C. Goonetilleke, R.E. Baltus, D. Roy, A Comparative Study of the Electrochemical Characteristics of [Emim][BF<sub>4</sub>] and [Bmim][BF<sub>4</sub>] Ionic Liquids at the Surfaces of Carbon Nanotube and Glassy Carbon Electrodes, *J. Phys. Chem. C* 115 (2011) 7527–7537.
- [13] L. He, Q. Xu, C. Hua, R. Song, Effect of multi-walled carbon nanotubes on crystallization, thermal, and mechanical properties of poly(vinylidene fluoride), *Polym. Compos.* (2010) 921-926.
- [14] T. Fukushima, A. Kosaka, Y. Ishimura, T. Yamamoto, T. Takigawa, N. Ishii, T. Aida, Molecular ordering of organic molten salts triggered by single-walled carbon nanotubes, *Science*, 300 (2003) 2072-2074.
- [15] J. M. P. França, C. A. Nieto de Castro, A. A.H. Pádua, Molecular Interactions and Thermal Transport in Ionic Liquids with Carbon Nanomaterials. *J. Name.*, 00 (2013) 1-3.
- [16] K. Asaka, Development of human-friendly polymeric actuators based on nano-carbon electrodes, *Synthesiology*, 9 (2016) 117-123.
- [17] Sugino, T.; Kiyohara, K.; Asaka, K, carbon nanotubes/Ionic liquid composites, In *Soft Actuators: Materials, Modelling, Applications, and Future Perspectives*, 2014. DOI.10.1007/978-4-431-54767-9\_9.
- [18] C. Espejo, F. J. Carri, D. Martinez, M. D. Bermudez, Multiwalled carbon nanotube-imidazolium tosylate ionic liquid lubricant, *Tribol. Lett.* 50 (2013) 127–136.
- [19] Y.K. Yang, L.J. Yu, R.G. Peng, Y.L. Huang, C.E. He, H.Y. Liu, X.B. Wang, X.L. Xie, Y.W. Mai, Incorporation of liquid-like multiwalled carbon nanotubes into an epoxy matrix by solvent-free processing, *Nanotechnology*, 23 (2012) e225701.
- [20] M.A. Salam, R. Burk, Synthesis and characterisation of multi-walled carbon nanotubes modified with octadecylamine and polyethylene glycol, *Arab. J. Chem.* 2013.<http://dx.doi.org/10.1016/j.arabjc.2012.12.028>

- [21] E.L.M. Pereira, A.S.M. Batista, F.A. S. Ribeiro, A.P. Santos, C.A. Furtado, L.O. Faria, Preliminary studies of MWCNT/PVDF polymer composites, *Int. J. Chem. Mol. Eng.* 10 (2016) 144-147.
- [22] T. Ohba, V. V. Chaban, A Highly Viscous Imidazolium Ionic Liquid inside Carbon Nanotubes, *J. Phys. Chem. B* 118 (2014) 6234-6240.
- [23] V.V. Chaban, O.V. Prezhdo, Nanoscale Carbon Greatly Enhances Mobility of a Highly Viscous Ionic Liquid, <http://pubs.acs.org>.
- [24] F. Taherkhani, B. Minofar, The Effect Of Nitrogen Doping On Glass Transition and Electrical Conductivity Of [EMIM][PF6] Ionic Liquid Encapsulated In Zigzag Carbon Nanotube, *J. Phys. Chem. C*, 2017. DOI: 10.1021/acs.jpcc.7b00911.
- [25] S. Chen, W. Guozhong, M. Sha, S. Huang, Transition of Ionic Liquid [bmim][PF6] from Liquid to High-Melting-Point Crystal When Confined in Multiwalled Carbon Nanotubes, *J. Am. Chem. Soc.* 129 (2007) 2416-2417.
- [26] T. Ohba, K. Hata, V. V. Chaban, Nanocrystallization of Imidazolium Ionic Liquid in Carbon Nanotubes, *J. Phys. Chem. C*, 2015. DOI: 10.1021/acs.jpcc.5b09423.
- [27] K. Subramanian, A. Das, G. Heinrich, Development of conducting polychloroprene rubber using imidazolium based ionic liquid modified multi-walled carbon nanotubes, *Compos. Sci. Technol.* 71 (2011) 1441-1449.
- [28] S. Bellayer, J. W. Gilman, N. Eidelman, S. Bourbigot, X. Flambard, D. M. Fox, H. C. De Long, P. C. Trulove, Preparation of homogeneously dispersed multiwalled carbon nanotube/polystyrene nanocomposites via melt extrusion using trialkyl imidazolium compatibilizer, *Adv. Funct. Mater.* 15 (2005) 910-916.
- [29] J. Wang, H. Chu, Y. Li, Why single-walled carbon nanotubes can be dispersed in imidazolium based ionic liquids, *ACS Nano* 2 (2008) 2540-2546.
- [30] C. A. Dyke, J. M. Tour, *J. Phys. Chem. A* 108(2004a) 11151; S. Banerjee, T. Hemraj-Benny, S. S. Wong, *Adv. Mater.* 17 (2005b)17; K. Balasubramanian, M. Burghard, *Small* 1 (2005c) 180; D. Tasis, N. Tagmatarchis, A. Bianco, M. Prato, *Chem. Rev.* 106 (2006d) 1105.
- [31] Ionic Liquids as Green Solvents?: ACS Symp. Ser. 2003, 856, ISBN13: 9780841238565. eISBN: 9780841219618. DOI: 10.1021/bk-2003-0856.
- [32] E. E. Fileti, V.V. Chaban, Imidazolium Ionic Liquid Helps to Disperse Fullerenes in Water. *J. Phys. Chem. Lett.*, 5 (2014) 1795-1800.
- [33] D.W. Lee, J. W.; Seo, Preparation of carbon nanotubes from graphite powder at room temperature, *Mater. Sci.* 4 (2011) 1-10.

- [34] X. Liu, J. Guo, J. Chen, J. Zhang, J. Zhang, Synergistic effect of ionic liquid intercalation and multiwalled carbon nanotube spacers with improved supercapacitor performance, *J. Power Sources*, 363 (2017) 54-60.
- [35] M. Tunckol, J. Durand, P. Serp, Carbon nanomaterial–ionic liquid hybrids, *Carbon*, 50 (4) 4303–4334.
- [36] T. Fukushima, A. Kosaka, Y. Ishimura, T. Yamamoto, T. Takigawa, N. Ishii, T. Aida, Molecular ordering of organic molten salts triggered by single-walled carbon nanotubes, *Science*, 300 (2003) 2072-2074.
- [37] L. Li, J. Groenewold, S.J. Picken, Transient phase-induced nucleation in ionic liquid crystals and size-frustrated thickening, *Chem. Mater.* 17 (2005) 250-257.

## Graphical abstract



ACCEPTED

**Highlights**

- Ionic liquids disperse carbon nanotubes without morphological alteration
- Ionic liquid-carbon nanotubes composites are more thermal stable than individual components
- Ionic liquid-functionalized carbon nanotubes composites are hydrophobic
- Non-covalent and Van der Waals interactions facilitate the ionic liquids/carbon nanotubes bonding